Electronic Supplementary Material (ESI) for New Journal of Chemistry.
This journal is © The Royal Society of Chemistry and the Centre National de la Recherche Scientifique 2015

Polyoxoanions assembled by condensation of Vanadate, Tungstate and Selenite: Solution Studies and Crystal Structures of Mixed Metal Derivatives $(NMe_4)_2Na_2[W^{VI}{}_4V^{V}{}_2O_{19}]\cdot 8H_2O$ and $(NMe_4)_{4.83}[(Se^{IV}W^{VI}{}_{4.57}V^{V}{}_{4.43}O_{33})_2(W^{VI}(O)(H_2O))(V^{V}O)_{2.6}]\cdot 10.57H_2O$

P.A. Abramov*,[a,b] E.V. Peresypkina,[a] N.V. Izarova,[c] C.Vicent,[d] A. Zhdanov,[a] N.B. Kompankov,[a] T. Gutsul,[e] M.N. Sokolov [a,b]

Supporting information

1) Crystal structures

Table S1. Crystallographic data for **1** and **2**.

Fig. S1. The numeration scheme in the structure of heterometallic $[(W_4V_2)O_{19}]^{4-}$ Lindqvist anion in $(NMe_4)_2Na_2[(W_4V_2)O_{19}]\cdot 8H_2O$.

Table S2. Selected geometric parameters (Å, º) in 1.

Fig. S2. The layer (top) and interposition of layers (bottom) in $(NMe_4)_2Na_2[(W_4V_2)O_{19}]\cdot 8H_2O$.

Fig. S3. The numeration scheme in the structure of heterometallic $[(Se(W_{4.57}/V_{4.43})O_{33})_2(W(O)(H_2O))(VO)_{2.6}]^{4.83-}$ in **2** (partial polyhedral view).

Table S3. Selected geometric parameters (Å, º) in **2.**

Fig. S4. The anion $[(Se(W_{4.57}/V_{4.43})O_{33})_2(W(O)(H_2O))(VO)_{2.6}]^{4.83-}$ (right) and crystal packing in $(NMe_4)_{4.83}[(Se(W_{4.57}/V_{4.43})O_{33})_2(W(O)(H_2O))(VO)_{2.6}]\cdot 10.57H_2O$ (left) (**2**, polyhedral view).

2) ESI-MS

Fig. S5. ESI mass spectrum of 10^{-4} M water solutions of sample **2** with 0.1 % of formic acid

Fig. S6. Expanded regions of the ESI mass spectrum of 10^{-4} M water solutions of sample **2** with 0.1 % of formic acid in the m/z 1150 to 1500 range where triply-charged anions are seen. Additional peaks featuring the central $\{WO(VO)_2\}$ belt were also observed for example at m/z 1338 $\{[(Se_2W_{11}V_7O_{66})\{WO(VO)_2\}\ +13H + 2K]^{3-}$ or 1293 $[(Se_2W_{10}V_8O_{66})\ \{WO(VO)_2\}\ +12H + 2K]3-$ but were overlapped with the dominant peaks due to POMs with the central $\{WO(VO)_3\}$ belt.

Fig. S7. Expanded region of the ESI mass spectrum of 10^{-4} M water solutions of sample **2** with 0.1 % of formic acid in the m/z 1850 to 2150 range (top) and simulated and experimental isotopic pattern for the indicated H+ adducts.

Fig. S8. Expanded region of the ESI mass spectrum of 10^{-4} M water solutions of sample **2** with 0.1 % of formic acid in m/z 1150 to 1500 range (top) and simulated and experimental isotopic pattern for the indicated H+ adducts.

Fig. S9. ^{51}V NMR spectra of initial mixture.

Fig. S10. ^{51}V NMR spectra of enriched product.

Fig. S11. ^{77}Se NMR spectra of enriched product.

Crystal structures.

Table S1. Crystallographic data for **1** and **2**.

Compound	**1**	**2**
Crystal data		
Chemical formula	$C_8H_{40}N_2Na_2O_{27}V_2W_4$	$C_{19.32}H_{81.10}N_{4.83}O_{81.17}Se_2V_{11.46}W_{10.14}$
M_r	1479.68	4286.10
Crystal system, space group	Orthorhombic, *Pnma*	Orthorhombic, *Pnn*2
Temperature (K)	150	150
a, *b*, *c* (Å)	18.6008(10), 9.9127(5), 18.2252(9)	19.4257(11), 21.2136(11), 12.9194(6)
V (Å^3)	3360.4(3)	5323.9(5)
Z	4	2
Radiation type	Mo *K*α	Cu *K*α
μ (mm^{-1})	14.29	29.32
Crystal size (mm)	0.266 × 0.185 × 0.138	0.10 × 0.10 × 0.05
Data collection		
Diffractometer	Bruker DUO CCD detector diffractometer	Bruker DUO CCD detector diffractometer
Absorption correction	Empirical (using intensity measurements) based on intensities (*SADABS*, Bruker, 2005)	Empirical (using intensity measurements) based on intensities (*SADABS*, Bruker, 2005)
T_{min}, T_{max}	0.0532, 0.0998	0.144, 0.320
No. of measured, independent and observed [$I > 2\sigma(I)$] reflections	23362, 4082, 3682	39238, 8396, 6877
R_{int}	0.0455	0.067
Refinement		
$R[F^2 > 2\sigma(F^2)]$, $wR(F^2)$, *S*	0.0513, 0.1095, 1.188	0.050, 0.146, 1.06
No. of reflections	4082	8396
No. of parameters	259	642
No. of restraints	0	1
$\Delta\rho_{max}$, $\Delta\rho_{min}$ (e Å^{-3})	2.870, -2.557	1.17, -2.59

Computer programs: Apex2 V.1.27 (Bruker, 2005), *SHELXS97* (Sheldrick, 1990), *SHELXL97* (Sheldrick, 1997), *SHELXTL* V6.22 (Bruker, 2000-2005), *SHELXL2013* (Sheldrick, 2013).

1) $(NMe_4)_2Na_2[(W_4V_2)O_{19}]\cdot 8H_2O$ (1)

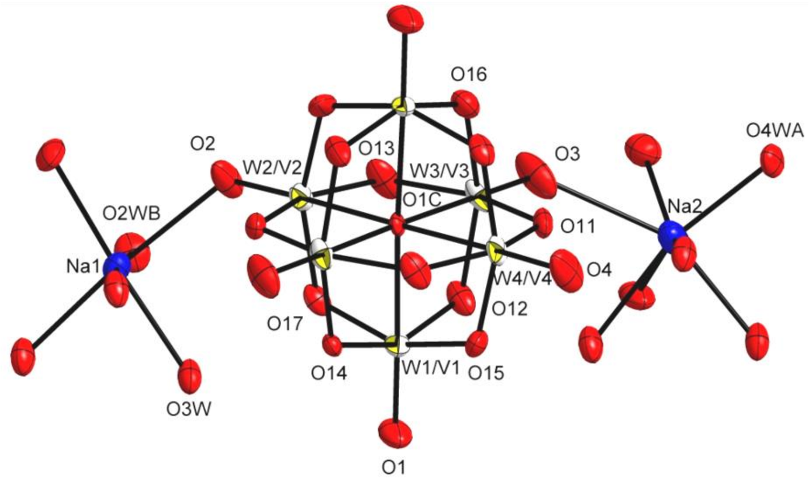

Fig. S1. The numeration scheme in the structure of heterometallic $[(W_4V_2)O_{19}]^{4-}$ Lindqvist anion in $(NMe_4)_2Na_2[(W_4V_2)O_{19}]\cdot 8H_2O$.

Table S2. Selected geometric parameters (Å, º) in **1**.

W1—O1	1.698 (8)	O4WA—Na2	2.29 (2)
W2—O2	1.710 (11)	O4WB—Na2	2.49 (4)
W3—O3	1.667 (8)	O5W—Na2	2.507 (18)
W4—O4	1.645 (12)	O2WA—Na1	2.33 (2)
W1—O12	1.913 (7)	O2WB—Na1	2.392 (17)
W1—O14	1.908 (5)	O3W—Na1	2.390 (9)
W1—O15	1.896 (7)	O3W—Na2^{ii}	2.427 (9)
W1—O17	1.935 (7)	O2—Na1	2.571 (13)
W2—O13	1.912 (8)	Na1—O2WA^{i}	2.33 (2)
W2—O13^{i}	1.912 (8)	Na1—O2WB^{i}	2.392 (17)
W2—O17^{i}	1.919 (7)	Na1—O3W^{i}	2.390 (9)
W2—O17	1.919 (7)	O1W—Na2^{ii}	2.496 (13)
W3—O11	1.901 (7)	Na2—O1W^{iv}	2.496 (13)
W3—O12	1.916 (8)	Na2—O3W^{iv}	2.427 (9)
W3—O13	1.922 (8)	Na2—O3W^{v}	2.427 (9)
W3—O16	1.905 (5)	Na2—O4WB^{iii}	2.49 (4)
W4—O11	1.881 (7)	Na2—O5W^{iii}	2.507 (18)
W4—O11^{i}	1.881 (7)	O1W—Na1	2.367 (13)
W4—O15^{i}	1.913 (8)	N1—C11	1.499 (18)
W4—O15	1.913 (8)	N1—C12	1.492 (18)
W4—O1C	2.308 (8)	N1—C13	1.480 (12)

W1—O1C	2.293 (6)	N1—C13^{iii}	1.480 (12)
W2—O1C	2.257 (8)	N2—C21	1.47 (2)
W3—O1C	2.287 (6)	N2—C22	1.480 (19)
		N2—C23	1.456 (17)
		N2—C23^{i}	1.456 (17)
W1^{i}—O1C—W1	89.9 (3)	W4—O11—W3	115.2 (3)
W1^{i}—O1C—W4	88.8 (3)	W1—O12—W3	115.7 (4)
W1—O1C—W4	88.8 (3)	W2—O13—W3	115.9 (4)
W2—O1C—W1^{i}	91.7 (2)	W1—O14—W1^{i}	116.2 (4)
W2—O1C—W1	91.7 (2)	W1—O15—W4	115.4 (3)
W2—O1C—W3	91.3 (3)	W3^{i}—O16—W3	115.7 (5)
W2—O1C—W3^{i}	91.3 (3)	W2—O17—W1	115.9 (3)
W3^{i}—O1C—W1^{i}	90.13 (2)	Range	115.2 (3)-116.2 (4)
W3—O1C—W1	90.13 (2)	W2—O1C—W4	179.2 (4)
W3—O1C—W3^{i}	89.7 (3)	W3—O1C—W1^{i}	176.9 (4)
W3—O1C—W4	88.1 (2)	W3^{i}—O1C—W1	176.9 (4)
W3^{i}—O1C—W4	88.1 (2)	Range	176.9 (4) -179.2 (4)
V3^{i}—O1C—V1^{i}	90.13 (2)		
Range	88.1 (2) - 91.7 (2)		

Symmetry code(s): (i) *x*, -*y*+1/2, *z*; (ii) -*x*+1/2, -*y*, *z*+1/2; (iii) *x*, -*y*-1/2, *z*; (iv) -*x*+1/2, -*y*, *z*-1/2; (v) -*x*+1/2, *y*-1/2, *z*-1/2.

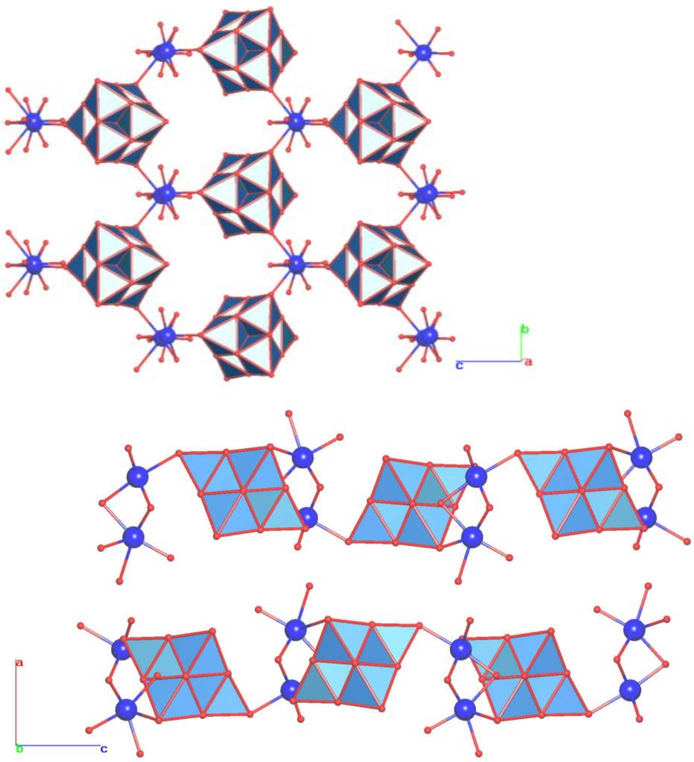

Fig. S2. The layer (top) and interposition of layers (bottom) in $(NMe_4)_2Na_2[(W_4V_2)O_{19}]\cdot 8H_2O$.

2) $(NMe_4)_{4.83}[(Se(W_{4.57}/V_{4.43})O_{33})_2(W(O)(H_2O))(VO)_{2.6}]\cdot 10.57H_2O$ (2)

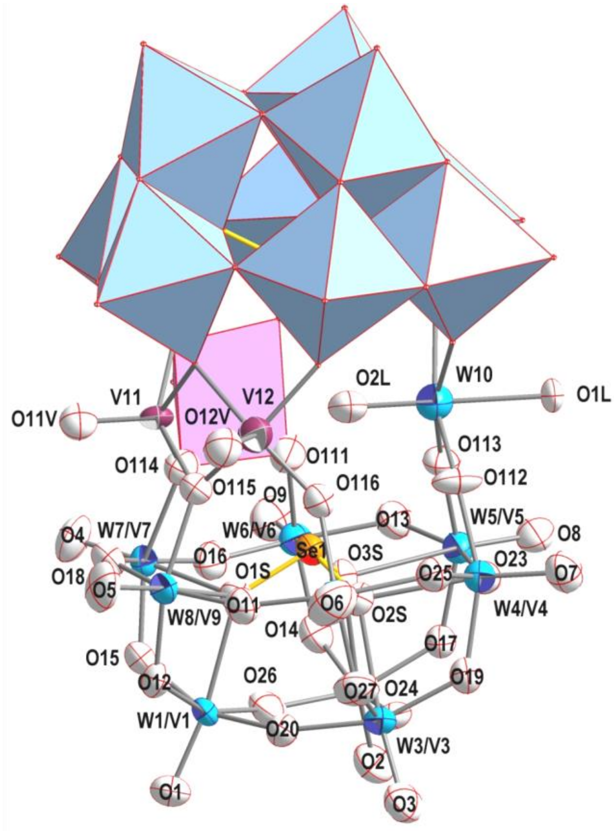

Fig. S3. The numeration scheme in the structure of heterometallic $[(Se(W_{4.57}/V_{4.43})O_{33})_2(W(O)(H_2O))(VO)_{2.6}]^{4.83-}$ in **2** (partial polyhedral view).

Table S3. Selected geometric parameters (Å, º) in **2.**

W1—O1	1.676 (18)	W4—O112	1.893 (15)
W2—O2	1.68 (2)	W5—O113	1.904 (16)
W3—O3	1.68 (2)	W6—O111	1.943 (17)
W4—O7	1.678 (19)	W7—O114	2.018 (18)
W5—O8	1.672 (19)	W8—O115	2.021 (17)
W6—O9	1.63 (2)	W9—O116	1.894 (15)
W7—O4	1.63 (2)	**W(O)(H_2O)**	
W8—O5	1.632 (19)	W10—O1L	2.28 (2)
W9—O6	1.64 (2)	W10—O2L	1.68 (3)
W1—O1S	2.320 (16)	W10—O113	1.896 (16)
W2—O3S	2.392 (16)	W10—O113^{i}	1.896 (16)
W3—O2S	2.382 (16)	W10—O112	1.898 (15)
W4—O2S	2.392 (16)	W10—O112^{i}	1.898 (16)
W5—O3S	2.381 (15)	**V-O**	

W6—O3S	2.333 (17)	V11—O11V	1.52 (4)
W9—O2S	2.377 (18)	V11—O115^{i}	1.920 (18)
W7—O1S	2.364 (17)	V11—O115	1.920 (18)
W8—O1S	2.379 (17)	V11—O114^{i}	1.97 (2)
W1—O20	1.878 (19)	V11—O114	1.97 (2)
W1—O12	1.913 (18)	V12—O12V	1.58 (2)
W1—O26	1.928 (19)	V12—O116	1.774 (17)
W1—O15	1.95 (2)	V12—O111^{i}	1.825 (19)
W2—O17	1.865 (16)	V12—O114^{i}	1.984 (19)
W2—O26	1.882 (18)	V12—O115	1.989 (19)
W2—O14	1.91 (2)	O111—V12^{i}	1.825 (19)
W2—O24	1.919 (18)	O114—V12^{i}	1.984 (19)
W3—O19	1.881 (17)	**Se-O**	
W3—O24	1.894 (19)	Se1—O2S	1.693 (16)
W3—O27	1.906 (19)	Se1—O1S	1.695 (16)
W3—O20	1.920 (17)	Se1—O3S	1.705 (17)
W4—O23	1.901 (18)	**N-C**	
W4—O19	1.927 (17)	N1—C13	1.45 (4)
W4—O25	1.929 (19)	N1—C11	1.48 (4)
W5—O23	1.866 (18)	N1—C14	1.49 (4)
W5—O17	1.898 (17)	N1—C12	1.54 (4)
W5—O13	1.905 (18)	N2—C24	1.42 (6)
W6—O16	1.834 (19)	N2—C21	1.43 (5)
W6—O14	1.878 (19)	N2—C23	1.47 (4)
W6—O13	1.938 (18)	N2—C22	1.50 (7)
W7—O15	1.868 (17)	N3—C34	1.39 (7)
W7—O16	1.87 (2)	N3—C31	1.41 (7)
W7—O18	1.93 (2)	N3—C32	1.46 (5)
W8—O11	1.82 (2)	N3—C33	1.46 (6)
W8—O12	1.893 (17)		
W8—O18	1.95 (2)		
W9—O27	1.892 (18)		
W9—O25	1.940 (18)		
W9—O11	1.877 (18)		
O2S—Se1—O1S	98.8 (8)	W6—O16—W7	156.6 (11)
O2S—Se1—O3S	99.4 (8)	W2—O17—W5	127.3 (9)
O1S—Se1—O3S	99.3 (8)	W7—O18—W8	122.2 (10)

W1—O1S—W7	90.6 (6)	W3—O19—W4	125.4 (9)
W1—O1S—W8	90.5 (5)	W1—O20—W3	149.3 (12)
W7—O1S—W8	91.3 (6)	W5—O23—W4	153.8 (10)
W9—O2S—W3	90.3 (6)	W3—O24—W2	147.7 (9)
W9—O2S—W4	91.3 (6)	W4—O25—W9	123.5 (10)
W3—O2S—W4	90.3 (5)	W2—O26—W1	148.8 (11)
W6—O3S—W5	92.4 (6)	W9—O27—W3	125.3 (9)
W6—O3S—W2	89.9 (6)	V12^{i}—O111—W6	140.6 (11)
W5—O3S—W2	89.9 (6)	W4—O112—W10	152.5 (11)
O11V—V11—O115^{i}	106.5 (6)	W10—O113—W5	153.2 (10)
O11V—V11—O115	106.5 (6)	V11—O114—V12^{i}	101.2 (8)
O115^{i}—V11—O115	146.9 (11)	V11—O114—W7	124.2 (10)
O11V—V11—O114^{i}	108.3 (6)	V12^{i}—O114—W7	131.6 (11)
O115^{i}—V11—O114^{i}	92.3 (8)	V11—O115—V12	102.7 (8)
O115—V11—O114^{i}	77.3 (8)	V11—O115—W8	124.9 (10)
O11V—V11—O114	108.3 (6)	V12—O115—W8	131.1 (10)
O115^{i}—V11—O114	77.3 (8)	V12—O116—W9	142.6 (10)
O115—V11—O114	92.3 (8)	C13—N1—C11	110 (2)
O114^{i}—V11—O114	143.4 (11)	C13—N1—C14	112 (2)
O12V—V12—O116	103.3 (9)	C11—N1—C14	110 (3)
O12V—V12—O111^{i}	104.1 (10)	C13—N1—C12	106 (3)
O116—V12—O111^{i}	94.7 (9)	C11—N1—C12	109 (3)
O12V—V12—O114^{i}	106.1 (9)	C14—N1—C12	110 (3)
O116—V12—O114^{i}	149.2 (8)	C24—N2—C21	116 (5)
O111^{i}—V12—O114^{i}	87.0 (8)	C24—N2—C23	109 (4)
O12V—V12—O115	105.1 (10)	C21—N2—C23	113 (3)
O116—V12—O115	88.3 (7)	C24—N2—C22	104 (4)
O111^{i}—V12—O115	149.2 (9)	C21—N2—C22	109 (5)
O114^{i}—V12—O115	75.4 (8)	C23—N2—C22	106 (4)
W8—O11—W9	155.9 (11)	C34—N3—C31	120 (5)
W8—O12—W1	122.5 (9)	C34—N3—C32	106 (4)
W5—O13—W6	124.7 (10)	C31—N3—C32	111 (4)
W6—O14—W2	123.7 (11)	C34—N3—C33	110 (4)
W7—O15—W1	121.1 (10)	C31—N3—C33	101 (4)
		C32—N3—C33	109 (4)

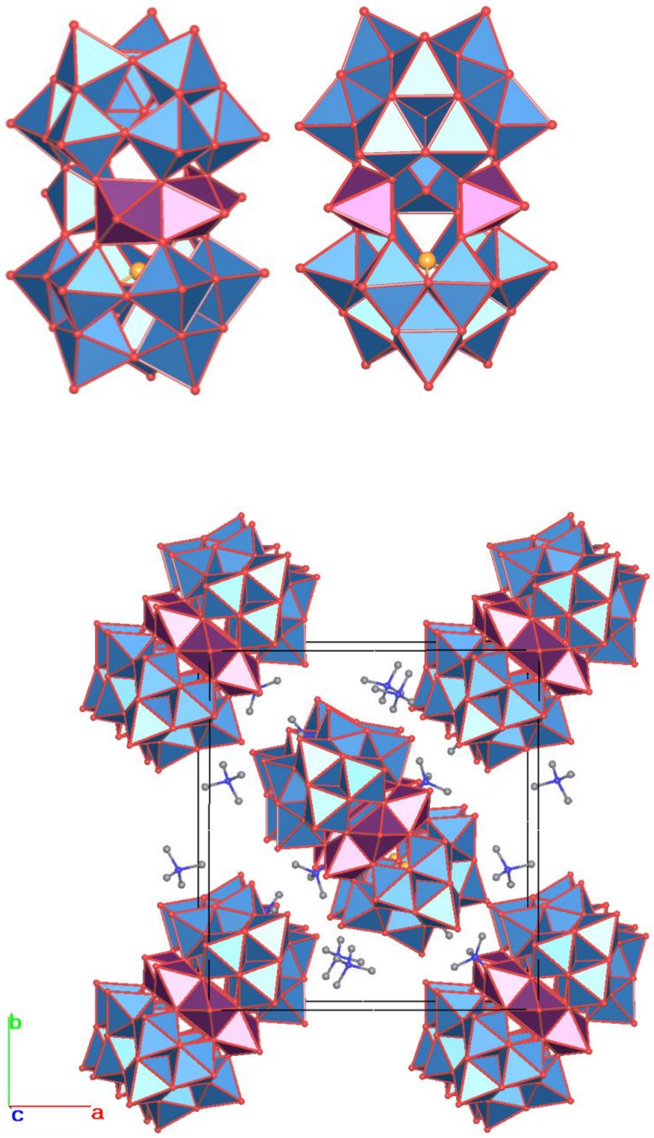

40% **+** **60%** **=** **co-crystal**

Fig. S4. The anion $[(Se(W_{4.57}/V_{4.43})O_{33})_2(W(O)(H_2O))(VO)_{2.6}]^{4.83-}$ (right) and crystal packing in $(NMe_4)_{4.83}[(Se(W_{4.57}/V_{4.43})O_{33})_2(W(O)(H_2O))(VO)_{2.6}]\cdot 10.57H_2O$ (left) (**2**, polyhedral view).

Table S4. Structural types of isolated complexes compounds.

Compound	a, b, c (Å)	α, β, γ (°)	Volume (Å^3)	Space group	POM type
Me2NH2+	8.595(1) 11.323(1) 16.133(2)	70.175(3) 87.075(3) 67.837(3)	1362.6(5)	$P\bar{1}$	$[(W/V)_6O_{19}]^{n-}$ (disordered)
Cs+	20.1143(4) 20.1143(4) 32.8320(15)	90.00 90.00 120.00	11503.7(6)	$R\bar{3}$	$[(Se(W/V)_9O_{33})_2(VO)_x(WO)_y]^{n-}$
Me2NH2+	34.382(2) 12.9291(9) 25.2008(17)	90 110.234(2) 90	10511.3(12)	C2/c	$[(Se(W/V)_9O_{33})_2(VO)_x(WO)_y]^{n-}$
Me2NH2+	41.0493(10) 41.0493(10) 36.4499(18)	90.00 90.00 120.00	53191(3)	$R\bar{3}$	$[(Se(W/V)_9O_{33})_2(VO)_x(WO)_y]^{n-}$
Me2NH2+	27.85(1) 27.86(1) 27.87(1)	107.53(1) 119.802(8) 99.52(1)	16545.3(4)	$P\bar{1}$	$[(Se(W/V)_9O_{33})_2(VO)_x(WO)_y]^{n-}$

2. SI-MS.

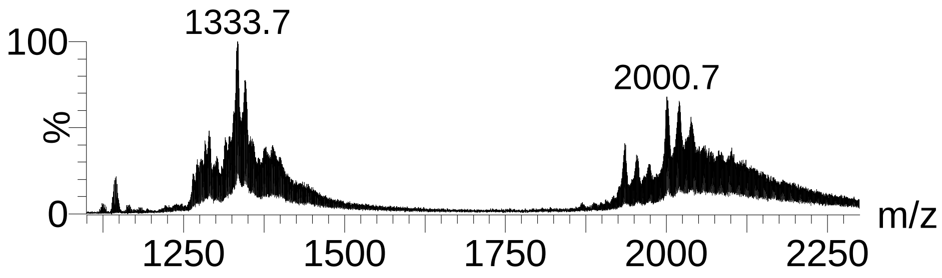

Fig. S5. ESI mass spectrum of 10^{-4} M water solutions of sample **2** with 0.1 % of formic acid

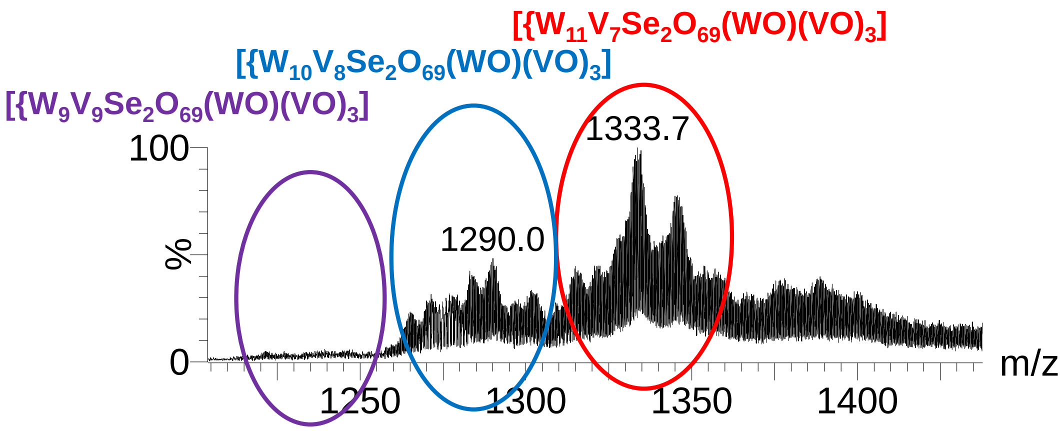

Fig. S6. Expanded regions of the ESI mass spectrum of 10^{-4} M water solutions of sample **2** with 0.1 % of formic acid in the m/z 1150 to 1500 range where triply-charged anions are seen. Additional peaks featuring the central {WO(VO)$_2$} belt were also observed for example at m/z 1338 {[(Se$_2$W$_{11}$V$_7$O$_{66}$){WO(VO)$_2$} +13H + 2K]$^{3-}$ or 1293 [(Se$_2$W$_{10}$V$_8$O$_{66}$) {WO(VO)$_2$} +12H + 2K]3- but were overlapped with the dominant peaks due to POMs with the central {WO(VO)$_3$} belt.

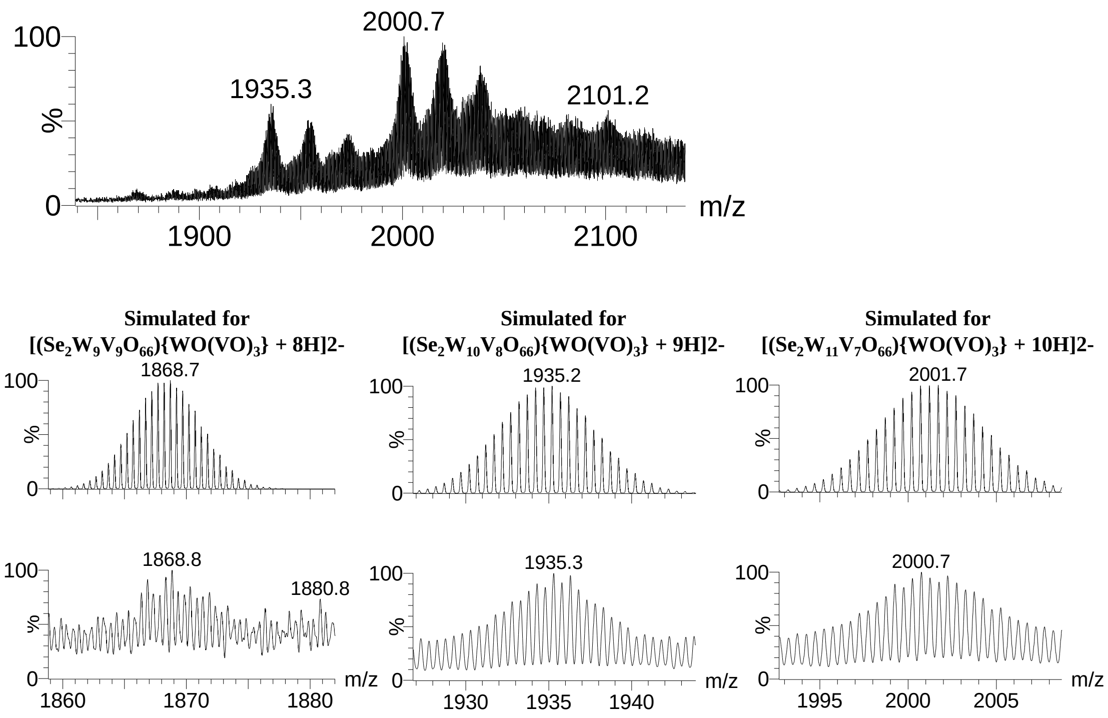

Fig. S7. Expanded region of the ESI mass spectrum of 10^{-4} M water solutions of sample **2** with 0.1 % of formic acid in the m/z 1850 to 2150 range (top) and simulated and experimental isotopic pattern for the indicated H+ adducts.

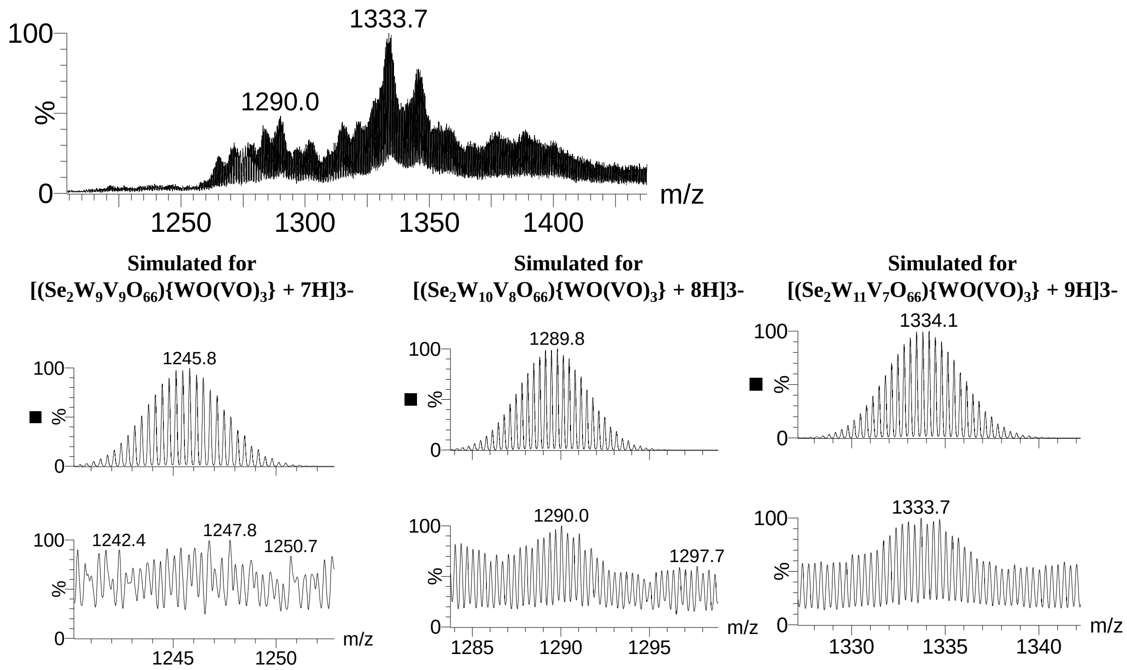

Fig. S8. Expanded region of the ESI mass spectrum of 10^{-4} M water solutions of sample **2** with 0.1 % of formic acid in m/z 1150 to 1500 range (top) and simulated and experimental isotopic pattern for the indicated H+ adducts.

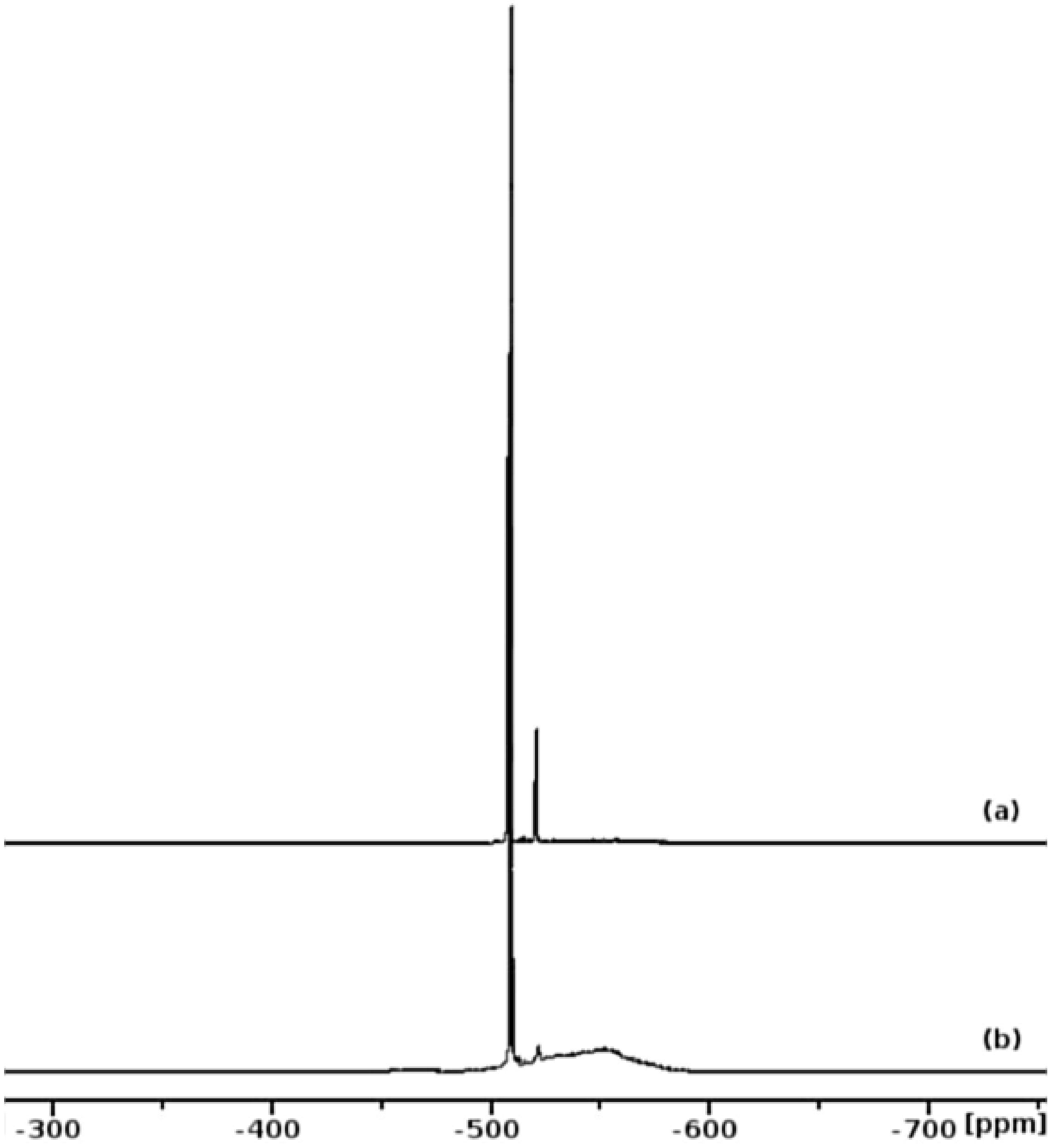

Fig. S9. ^{51}V NMR spectra of initial mixture.

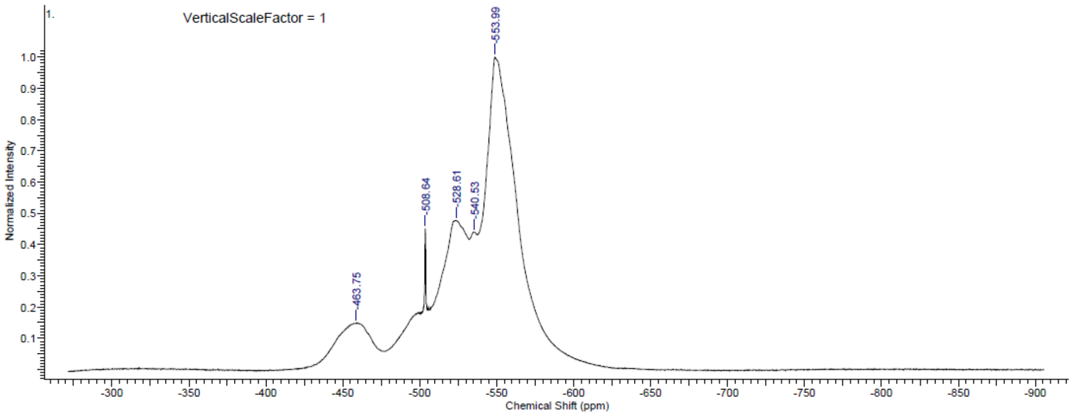

No.	(ppm)	(Hz)	Height
1	-553.99	-43699.0	1.0000
2	-540.53	-42636.7	0.4403
3	-528.61	-41696.5	0.4776
4	-508.64	-40121.4	0.4514
5	-463.75	-36580.4	0.1490

Fig. S10. ^{51}V NMR spectra of enriched product.

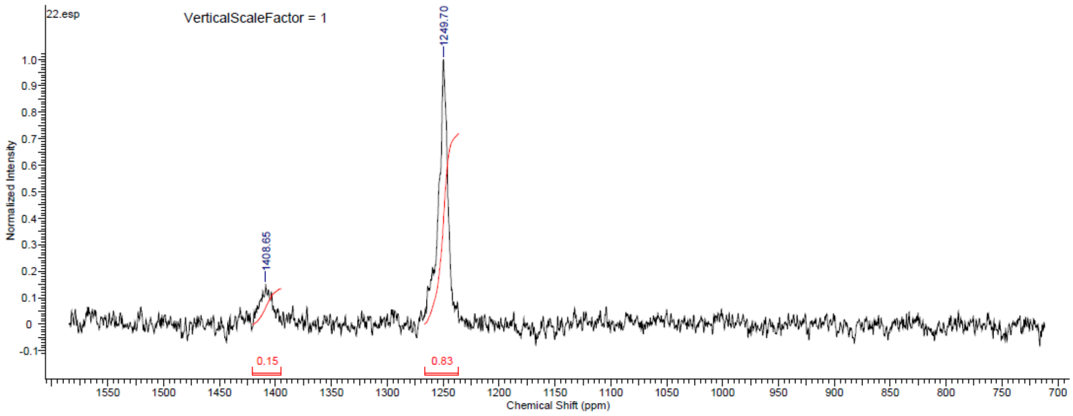

Fig. S11. ^{77}Se NMR spectra of enriched product.